Aeolian Research 50 (2021) 100677

Contents lists available at ScienceDirect

Aeolian Research

journal homepage: www.elsevier.com/locate/aeolia

Influence of mineral dust on the concentration and composition of PM10 in the city of Constantine

Kanza Lokorai [a], Hocine Ali-Khodja [a,*], Salah Khardi [b], Fairouz Bencharif-Madani [a], Lamri Naidja [a,c,d], Mokhtar Bouziane [a]

[a] Laboratoire de Pollution et Traitement des Eaux, Département de Chimie, Faculté des Sciences Exactes, Université Frères Mentouri-Constantine 1, Constantine, Algeria
[b] Université Claude Bernard - IFSTTAR LTE, 25, Avenue François Mitterrand, Case 24 Cité des Mobilités, F-69675 Bron Cedex, France
[c] Centre de Recherche Scientifique et Technique en Analyses Physico-Chimiques (CRAPC), BP 384, Siège ex Pasna Zone Industrielle Bou-Ismail, CP 42004 Tipaza, Algeria
[d] Centre de Recherche en Sciences Pharmaceutiques, Zone d'activité ZAM, Nouvelle Ville Ali Mendjli, Constantine, Algeria

ARTICLE INFO

Keywords:
PM10
Mineral dust
Saharan dust
Metallic elements
Back trajectories

ABSTRACT

Measurements of Saharan dust (SD) inputs are very scarce in the vicinity of the Saharan desert. This work aims to identify Saharan dust intrusions and evaluate their contribution to annual and daily PM10 at an urban background site located in the city of Constantine in Algeria. A reliable identification of SD days was carried out using aerosol maps provided by BSC-DREAM model and the information provided by HYSPLIT air mass back trajectories. SD is mainly composed of mineral dust (MD) due to the proximity of the Sahara to the study site. MD was determined by chemical speciation analysis and was estimated on SD days and non SD days. The contribution of MD on SD days was about 50% higher than that observed on non SD days. The observed average PM10 concentration during the study period was 56 ± 32.0 μg/m^3. During SD days, the average PM10 concentration was 70 ± 36.1 μg/m^3. On average, the PM10 concentration increased by 17.05 ± 12.7 μg/m^3 on SD days. SD events contributed between 0.6 and 41.5 μg/m^3 to the daily PM10 concentrations, whereas the average contribution to the annual PM10 concentration was 7.2 ± 11.8 μg/m^3 i.e., 12.8 ± 15.5%. After the extraction of the SD load, the annual WHO air quality guideline (AQG) was still exceeded. SD incursions led to an increase of most metal elements concentrations by a factor ranging from 1.05 to 3.33. Our results point out that SD outbreaks are quite frequent as they occurred 42.2% of the annual days.

1. Introduction

In North Africa, the Sahara is responsible for half of the MD emissions globally and is known as the major aeolian source of MD in the entire world (Aleksandropoulou and Lazaridis, 2013). Mineral dust is mainly Saharan dust because of the geographical proximity of the desert to northern Algeria (Bouet et al., 2019). Most of the SD is deposited in the region of generation. According to Naidja et al. (2018), out of 715.8 million t originating from North Africa, 608.2 t was deposited over the continent. SD is transported every year towards North African countries, the Mediterranean Sea and south European countries (Barkan et al., 2005). The proximity of the Algerian city of Constantine to the Sahara exacerbates the impact of desert dust events on ground level aerosol load. MD can be originated from other sources such as agricultural activities, local soil resuspension, construction or demolition works, driving over unpaved roads and traffic-induced resuspension (Denier, 2000; Valido et al., 2018). The composition of PM10 is greatly affected by contributions from natural sources, with concentration levels specifically high during episodes of SD intrusions (Jiménez et al., 2010). Effectively, dust may increase significantly the atmospheric levels of PM, adversely affecting air quality (Marconi et al., 2014).

When MD is produced in big quantities, it generates dust storms which impact negatively air quality and human health (Maghrabi and Al-Dosari, 2016) and leads to damages to the flora and fauna, depending on its mineralogical composition (Schepanski, 2009). Dust storms cause harm to agricultural crops and a reduction in soil fertility. They produce atmospheric instabilities and affect chemical and biological ecosystems (Maghrabi and Al-Dosari, 2016) and also impact radiation and cloud

* Corresponding author.
E-mail addresses: lokoraikanza@hotmail.com (K. Lokorai), halikhodja@umc.edu.dz, hocine_ak@yahoo.fr (H. Ali-Khodja), salah.khardi@univ-eiffel.fr (S. Khardi), fbencharifmadani@gmail.com (F. Bencharif-Madani), lamri.naidja@gmail.com (L. Naidja), mokhtar.bouziane@univ-msila.dz (M. Bouziane).

https://doi.org/10.1016/j.aeolia.2021.100677
Received 28 August 2020; Received in revised form 11 January 2021; Accepted 11 January 2021
Available online 2 February 2021

microphysics (Schepanski, 2009).

Daily PM10 levels recorded at seven monitoring stations in the Tunisian coasts during desert dust episodes reached 700 μg/m^3 and were much higher than the average levels during non-desert dust episodes (up to 100 μg/m^3) (Terrouche et al., 2015).

The size and shape of dust particles have a direct relation with their influence on environmental impacts. Primarily, the coarse particles are deposited near the source regions, but finer particles can be elevated 6–7 km above the ground and transported by synoptic circulation systems over long distances, up to thousands of kilometers and to different directions from their emission source (Gobbi et al., 2007; Thorsteinsson et al., 2011; Knippertz, 2014), often in large quantities (Goudie, 2014). This can be explained by the quick injections of dust particles into the free troposphere produced by strong winds and intense convective activity in arid regions (Gobbi et al., 2007).

It has been demonstrated that MD aerosols contribute to the exceedance of the daily mean WHO AQG of 50 μg/m^3 for PM10 mainly due to episodes of SD outbreaks and also soil dust resuspension at local and regional scales (Perez et al., 2012; Salvador et al., 2013) in many European countries such as Spain (Rodriguez et al., 2001), Greece (Gerasopoulos et al., 2006), Italy (Matassoni et al., 2011) and others. Thus, several studies investigated the influence of African MD on air quality, mainly on PM10 and PM2.5, in Mediterranean countries such as Tunisia (Bouet et al., 2019; Chtiouiet al., 2019; Kchih et al., 2015) and European cities (Rodríguez et al., 2001; Querol et al., 2009; Remoundaki et al., 2011; Aleksandropoulou and Lazaridis, 2013; Salvador et al., 2013; Pey et al., 2013; Kabatas et al., 2014). Intensity and frequency of dust outbreaks have been widely investigated in Southern European countries.

Algeria is the largest African country encompassing a large fraction of the Sahara. The Algerian Sahara covers 2 million km^2 which represents 80% of the country and 25% of the total area of this great desert that crosses ten countries from Egypt to Mauritania. North Africa is among the most affected areas by global dust storms in the world and its desert is the largest contributor to the global dust burden (50–70%) (Guan et al., 2019). North African cities are more affected than European ones by the transport and contribution of SD because of their geographical proximity to the Sahara. Nevertheless, very few studies on SD have been carried out in Africa (De Longueville et al., 2013). Mineral dust has never been the subject of research in Algeria. It is thus important to quantify the contribution of natural sources to PM10 for air quality assessment and in order to evaluate the effectiveness of air pollution control measures (Wang et al., 2018; Guan et al., 2019).

For the first time, this work aims to assess the contribution of MD to the concentration levels and chemical composition of airborne PM10 as well as to the daily WHO AQG exceedances (WHO, 2016), at an urban monitoring site in the south of the city of Constantine during the period extending from January 2015 to January 2016. Moreover, it compares concentrations of PM10 and metallic elements on days with and without SD intrusions. A reliable identification of Saharan dust (SD) episodes at the study site was carried out based on BSC-DREAM images and HYSPLIT (Hybrid Single Particle Lagrangian Integrated Trajectory Model) air mass back trajectories. Moreover, this study aims at determining the percentage of SD events and their contribution to the levels and chemical composition of PM10 during SD days and non SD days, in Constantine.

2. Materials and methods

2.1. Site description

Algeria is a Northern African country with a coastline on the Mediterranean Sea and a desert interior, the Sahara. Constantine is the third most important city of the country and is located in the North East with an area of 2197 km^2 and 450,000 inhabitants (Fig. 1). Constantine has a warm Mediterranean climate with hot and dry summer. Its climate is characterized by a cold period (-2–12 °C) with significant rainfall (500–700 mm/year) between October and March and a warm and rather dry period (25–45 °C) between April and September. Constantine is situated between the Mediterranean Sea and the Sahara desert. During the cold period, predominant winds are north–north-westerly mainly due to the North Atlantic advection, while during the hot period, winds are south-south-easterly mainly due to Sirocco winds.

The sampling site was located south of Constantine within the Faculty of Earth Sciences at the Zouaghi area (36°22′N, 6°40′E, 721 m.a.s.l), about 200 m from National Road N° 79, which is one of the busiest traffic highways in the city (Fig. 1). The sampling device was located

Fig. 1. Geographical location of Algeria and Constantine, the location of the sampling site and the volume air sampler used.

about 3 m above the ground, at an urban site fully exposed to winds and free all around of other obstacles (Remoundaki et al., 2011).

2.2. PM10 sample collection

Sampling was scheduled at midnight for 24 h every 6 days during one year from 15 January 2015 to 3 February 2016. A total of 64 samples were collected during the measurement campaign. A high volume air sampler (Tisch Environmental, model TE-6070) was used with a flow-rate in the range 1.04 – 1.24 m^3/h. Hourly meteorological data from the nearby meteorological weather station of Ain-El-Bey which is located 1.5 km to the south of the sampling site were used. PM10 samples were trapped by quartz microfiber filters (25 cm × 20 cm). Before and after each sampling interval, the collection media were humidity and temperature stabilized for 48 h before weighing them to a precision less than ± 0.01 mg using a Shimadzu balance (model AUW120D).

2.3. Acid digestion procedure

The acidic digestion procedure chosen was based on the method proposed by Querol, 2001. According to Kemmouche et al. (2017), this digestion procedure allows the highest recovery yields of most of the mineral part present in alumino-silicates rich filters. The samples were digested in an acidic mixture containing 1 mL HNO_3 and 2 mL HF in closed PFA flasks at 90 °C for 8 h. After cooling, 1 mL $HClO_4$ was then added. For complete evaporation, the PFA bombs were placed on a hot plate at 240 °C. The final dry residue was dissolved in 2.5 mL HNO_3 and brought to 25 mL of distilled Milli-Q water. Blank concentrations were on average 3.6% (for major elements) and 5.4% (for trace elements). They were, of course, subtracted from sampler filter concentrations.

2.4. Analytical techniques

All the obtained solutions from PM10 and blank filters were analyzed by ICP-AES (IRIS Solutions Advantage Thermo TJA) for Al, Ca, Fe, K, Mg and Na and by ICP-MS (X Series II Thermo) for Li, Be, Ba, Cu, Bi, Mn, S, P, V, Ni, Zn, Pb, Sr, Ti, V, Cr, Co, Ga, Ge, As, Se, Sr, Y, Zr, Nb, Sn, La, Ce, Pr, Nd, Sm, Cd, Gd, Dy, Hf, Ta, W, Th, U, Sb, Sc and Rb. To check the accuracy of the analytical procedure, a Nist 1633b (fly ash) mineral-rich reference material was subjected to the same digestion protocol and then analyzed. Extraction yields of metal elements ranged from 97% to 117% (in most cases falling into the uncertainty given for them in the certifications. Such results can be considered very satisfactory in terms of elemental recoveries. All PM10 samples were analyzed for their elemental composition at IDAEA-CSIC laboratory in Barcelona.

2.5. Determination of dust episodes

In order to identify the days affected by Saharan dust intrusions in Constantine during the study period, we used the same methodology proposed and employed in several European studies (Escudero et al., 2005, 2007a, 2007b; Querol et al., 2009; Pey et al., 2010, 2013a, 2013b; Salvador et al., 2014; Pandolfi et al., 2014; Stafoggia et al., 2016). Such an approach consists in identifying African dust intrusions for each sampling day at any location, regardless of their intensity. The methodology is based on a combination of modeling tools and meteorological information, by using:

Aerosol maps: BSC-DREAM8b (Dust REgional Atmospheric Model) dust maps: https://ess.bsc.es/bsc-dust-daily-forecast);. Simulation with this system was carried out for all sampling days.

Back-trajectories of air masses using the HYSPLIT model (HYbrid Single-Particle Lagrangian Integrated Trajectory) (HYSPLIT: https://ready.arl.noaa.gov/HYSPLIT.php). 5-days back-trajectories were computed ending at 12 h GMT at altitudes of 750, 1500 and 2500 m.a.s.l. (above sea level), in order to examine the entire depth of the planetary boundary layer (PBL) (Matassoni et al., 2009). The three altitudes are appropriate for identifying SD transport events and correspond to transport at surface, boundary layer height and free troposphere (Aleksandropoulou and Lazaridis, 2013). Back-trajectories were used to support SD intrusions identified by BSC-DREAM8b.

Potential Saharan dust (SD) transport events in Constantine were detected using the BSC-DREAM8b model maps providing information on ground dust concentrations and the HYSPLIT model for back-trajectories (Guan et al., 2019).

BSC-DREAM8b maps were first evaluated and whenever they indicated the presence of SD. Then, back-trajectories were interpreted to confirm the transport of air masses from the Sahara. There was a good agreement between the transport patterns obtained from BSC-DREAM8b and air back-trajectories for all SD events.

For some days, the presence of SD is not always reflected by back-trajectories or BSC-DREAM8b models simultaneously. This is due to the fact that SD is sometimes trapped in the atmosphere because of favorable meteorological conditions such as vertical stability, persistent anticyclonic conditions, lack of rainwater and very weak winds (Querol et al., 2009). In these cases, SD continues to affect PM10 levels often from 1 to 3 days after the intrusion before falling to the ground by dry or wet deposition (European Commission, 2011; Pey et al., 2013a, 2013b; Aleksandropoulou and Lazaridis, 2013).

On a total of 64 days of the measurement campaign, 27 SD days were detected in the city of Constantine. Examples of back-trajectories and aerosol maps are shown in Fig. 2 for days with high SD inputs.

2.6. Dust empirical equation

There exists a variety of empirical methods for calculating the contribution of MD to PM from elemental constituents considered to be associated with crustal material (Loy et al., 2000; Denier, 2007; Remoundaki et al., 2011; European Commission, 2011; Rodríguez et al., 2011; Miller-Schulze et al., 2015; Perrone et al., 2016).

To investigate the mass contribution of MD to PM10 from elemental constituents usually associated with crustal origin, we converted the elements to their common oxide form using the model of Remoundaki et al. (2011), in Equation (1).

$$\text{Mineral Dust Oxide} = [SiO_2] + [Al_2O_3] + [Fe_2O_3] + [CaO + CaCO_3] + [K_2O] + [MgO] + [TiO_2] \quad (1)$$

Silicon was not analyzed because the quartz filters are rich in this element. SiO_2 was, however, estimated as follows: $[SiO_2] = 3 \times [Al_2O_3]$ (Alastuey, 2005).

To estimate the calcium levels in its most abundant forms ($CaO + CaCO_3$), Ca was multiplied by a factor of 1.95. $[CaO + CaCO_3] = 1.95 * [Ca]$ (Remoundaki et al., 2011).

Mineral dust is mainly due to SD intrusions but it also results from the contribution of soil dust resuspension on a local scale (Perez et al., 2012; Salvador et al., 2013). Local dust emissions can be significant due to the proximity of bare soil to the sampling site. Silty soil is only 300 m to the west and 600 m to the north and to the east of the study station.

2.7. Enrichment factor

In order to delineate the anthropogenic or crustal origins of trace metals in atmospheric aerosols, average enrichment factors (EF) with respect to Al have been estimated in PM10 at the monitoring site (Sudheer and Rengarajan, 2012). EF represents the ratio of elemental concentrations in the aerosol samples normalized to crustal concentrations. Al is commonly used as a crustal source indicator and EFx are calculated by using equation (2):

$$EFx = (Cx/CAl)_{sample}/(Cx/CAl)_{crust} \quad (2)$$

Where C*x* and C*Al* are concentrations of the element × and *Al* in samples and Cx_{crust} and CAl_{crust} are average crustal concentrations

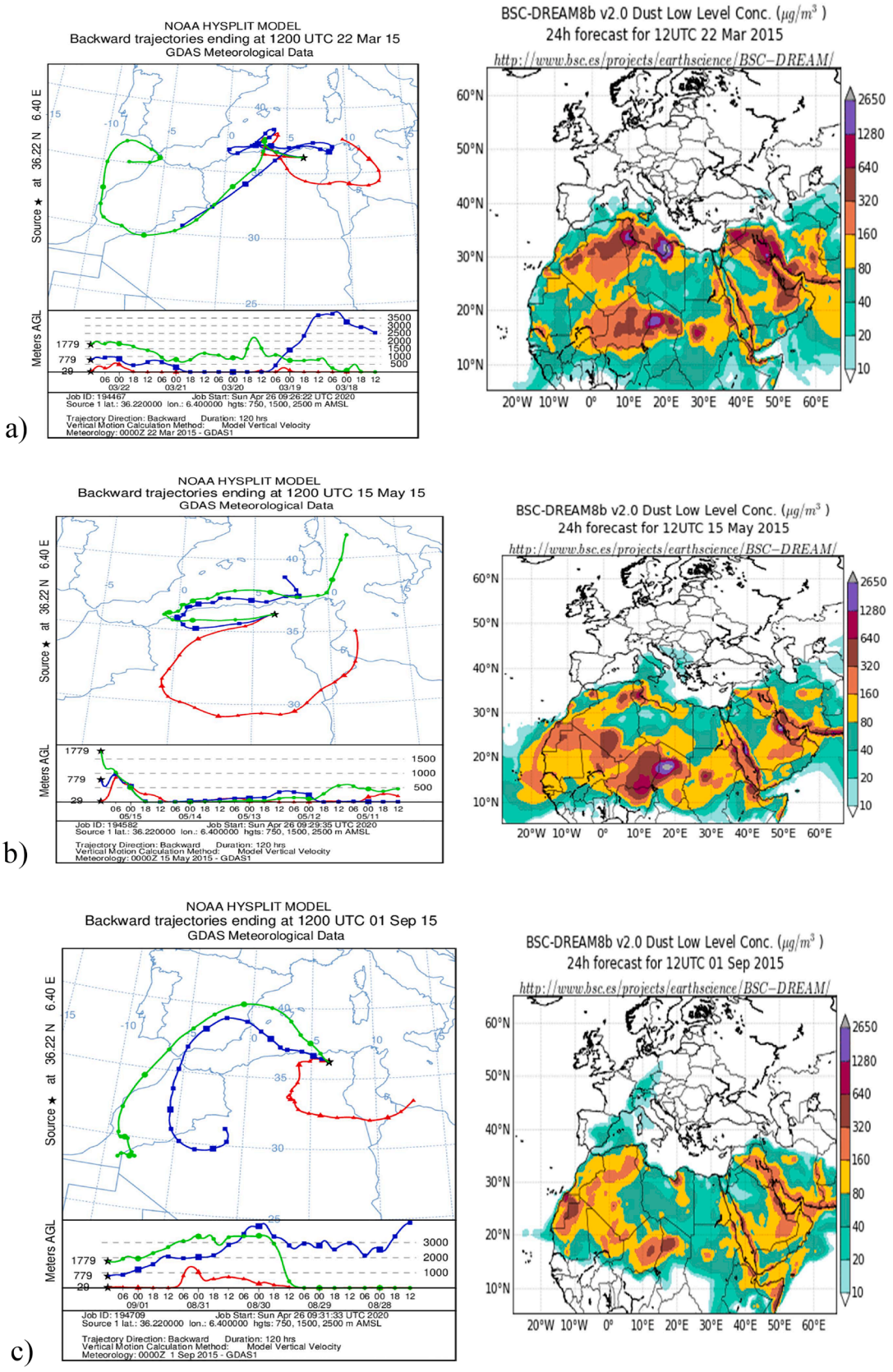

Fig. 2. Saharan dust days detected by HYSPLIT and BSC-DREAM8b in Constantine on: a) 22/03/2015, b) 15/05/2015 and c) 01/09/2015.

(Taylor and McLennan, 1995). This calculation assumes that the contribution of anthropogenic Al is not significant at the sampling area. If EF approaches 1, crustal sources are predominant and generally a value > 5 indicates a large fraction can be attributed to anthropogenic sources. If EF exceeds 100, sources are mainly anthropogenic.

3. Results and discussion

3.1. Identification of Saharan dust days

Table 1 summarizes some statistical data relating to SD events. The WHO 24-h AQG value was exceeded on 33 days, which is 51.5% of the sampling days. The number of measurement days impacted by SD was 27 (class "b" in Table 1). Of these 27 dusty days, 19 exceedance days were identified as being impacted by SD. In other words, 14 exceedance days were identified in non SD days (class "d"). The number of violations due to SD input was 4 (class "e"). In other terms, the absence of SD would have resulted in acceptable daily PM concentrations. Class "f" days would still be exceedance ones even in the absence of SD.

In approximately 40% of SD days, the estimated MD input to PM10 was < 10 μg/m^3 and the corresponding percentage contribution was in the range 2.3%-26.9%.

3.2. Influence of SD outbreaks on PM10 and MD concentrations levels

Table 2 reports the concentrations of PM10 and MD on SD days identified by the methodology described in section 2.5. Daily mean PM10 levels were > 30 μg/m^3 in the 85% of the SD episodes and > 50 μg/m^3 in the 70% of these events. The total number of SD days identified throughout the whole year according to this methodology was 155 (42.5% days/year) for a total number of 40 episodes/year. An episode encompasses all successive days with SD advections. For the same period, on a total of 64 sampling days, 27 days were affected by SD intrusions. The percentage of SD days was 42.2%. The latter was therefore representative of the whole year in terms of percentage of SD occurrences. During this campaign, thirty-three daily exceedances with regard to the WHO AQG (50 μg/m^3) were detected. For the following dates : 20/02/2015, 19/8/2015, 25/8/2015, 18/9/2015 and 30/9/2015, the modeled dust surface concentrations were overestimated in comparison with calculated MD. Such an overestimation has been reported by Monteiro et al (2015) for dust activity in Northern Algeria.

The concentration profiles of PM10 and MD varied quite similarly (Fig. 3). MD affects and contributes significantly to PM10 concentrations. During SD days, daily percentage mass contributions of MD in Constantine varied from a minimum of 2.3% to a maximum of 62.8% to PM10 with an average of 24.2% as shown in Table 2 which also indicates elemental ratios. Throughout the whole year, the contribution of SD to the annual average PM10 concentration was 7.2 μg/m^3. The substraction of SD solely during desert outbreaks would lead to a reduction of 12.83% of the annual PM10 concentration which would be 48.8 μg/m^3.

Table 2 shows that air masses identified as Saharan dust incursions originate mainly from the SW and SE directions and less frequently in the NW, S and NE sectors.

In Constantine, MD contributed 21.23% to PM10 in mass during the whole sampling period, 24.25% during SD intrusions and 17.52% in the absence of SD outbreaks (Table 3). The average concentration of MD during the whole sampling campaign was 11.89 μg/m^3. The subtraction of the contribution of total MD representing mainly the sum of soil resuspension, long-range transport SD and traffic-induced resuspension would lead to an annual average PM10 concentration of 44.12 μg/m^3. Such a value was 21.21% lower than the observed annual PM10 concentration.

On average, the PM10 concentration increased by 17.05 μg/m^3 on SD days. Such a value was higher than the overall increase observed on SD days in the 11 European cities of the MED-PARTICLES project which reached 13.4 μg/m^3 (Staffogia et al., 2016).

Table 1
Statistical data relating to Saharan Dust (SD) events.

Total number of sampling days	64
a. Number of violations	33
b. Number of days affected by SD intrusions	27
c. Number of SD days violations	19
d. Number of violations in non SD days	14
e. Number violations due to SD	04
f. Number of violations not due to SD	29

3.3. PM10 and MD temporal variability and influence of meteorological parameters

The observed average PM10 concentration during the study period was 56.0 μg/m^3. Minimum and maximum values were 5.0 μg /m^3 and 136 μg /m^3 respectively. Such an average value was less than levels reported by Talbi et al. (2017) in Algiers, the capital of Algeria in 2015 (61.38 μg/m^3) and by Flores et al. (2017) in Istanbul (Turkey) in 2013 (73.9 μg/m^3) but higher compared to levels observed by Bouet et al. (2019) in Tunisia in 2015 (44 μg/m^3) and by Diapouli et al. (2017) in 2013/2014 in five Mediterranean European countries in Porto (34.6 μg/m^3), Barcelona (22.5 μg/m^3), Milan (35.8 μg/m^3), Florence (19.8 μg/m^3) and Athens (19.6 μg/m^3).

Fig. 3 shows the temporal variability of the average daily PM10 and MD concentrations as well as average daily precipitation during the sampling period. The WHO daily AQG of 50 μg/m^3 is represented by a red line.

The lowest observed PM10 concentrations coincided with the highest precipitation rates during this period. PM10 concentrations exceeding 100 μg/m^3 were observed on the following dates: 01/09/2015 (107 μg/m^3), 15/04/2015 (114 μg/m^3), 03/05/2015 (128 μg/m^3), 15/05/2015 (126 μg/m^3), 06/10/2015 (128 μg/m^3) and 17/12/2015 (136 μg/m^3) whose MD contributions varied between 18.4% and 32.3%.

The frequency of occurrence of SD within seasons was in descending order: summer (60%), autumn (40%), spring (37.5%) and winter (33%). Although summer events were more frequent, the highest average contribution of MD to PM10 was observed in spring, while the lowest was recorded in autumn. The mean contribution of MD to PM10 was 12.1% in autumn but reached 28.8%, 27.5% and 23.5%, in spring, summer and winter respectively. There was no significant seasonality between summer and winter MD inputs (Fig. 4) as precipitation levels were exceptionally scarce during the rainy season in 2015 compared with the long term rainfall average which is of the order of 630 mm. According to Israelevich et al. (2002) and Schepanski (2009), the atmosphere over North Africa is almost constantly loaded with a significant amount of MD in spring and summer. Referring to Israelevich, et al. (2002), it is natural that the spring and summer seasons have a more significant part of MD because the trajectory of transport of SD is in the direction of North Africa and the Mediterranean Sea. According to Dulac et al. (1997) the seasonal desert dust transport patterns of North Africa indicate a maximum desert load in the eastern Mediterranean basin during spring and in the central and western basin during summer.

MD is always more or less present in PM even outside SD days. This is due to soil resuspension of MD and/or the persistence of SD in the air after outbreaks vanish due to certain meteorological conditions (2014;; Escudero et al., 2007b).

Above-limit daily PM10 concentrations are reported in Fig. 3. The observed average PM10 concentration over the study period exceeded the WHO annual recommended limit value

(20 μg/m^3) by a factor of 2.75. This can, partly, be explained by the exceptional scarcity of observed precipitation during the study period as total rainfall amounted to only 199.5 mm. When the soil is dry and the meteorological conditions are favorable (low humidity and presence of

Table 2
PM10 and MD concentrations (μg/m^3) during SD days identified by the HYSPLIT model, relative proportion of MD in PM10, air mass origins and elemental ratios.

Date	PM10*	MD	% contribution	Air mass origins**			Ca/Al	Fe/Ca	K/Ca	Mg/Al	(Ca + Mg)/Fe
				750	1500	2500					
15/01/2015	55.7	35.0	62.8	SW	SW	SW	9.8	0.07	0.03	0.36	14.6
21/01/2015	29.6	16.5	55.7	SW	SW	SW	13.9	0.07	0.02	0.67	15.0
20/02/2015	13.0	3.5	26.9	SE	SE	SE	11.1	0.10	0.05	0.86	10.8
04/03/2015	54.0	26.1	48.3	SW	SW	SW	13.2	0.07	0.08	0.58	14.3
22/03/2015	78.6	24.9	31.7	SE	SE	SW	3.2	0.18	0.09	0.34	6.2
15/04/2015	114.2	36.9	32.3	SE	NW	NW	6.0	0.10	0.05	0.39	10.8
03/05/2015	128.3	41.5	32.3	SE	SW	S	5.9	0.10	0.05	0.40	10.6
15/05/2015	126.2	35.5	28.1	SE	NE	NE	6.0	0.10	0.05	0.40	11.2
08/06/2015	78.6	22.1	28.1	SE	SE	SE	6.4	0.10	0.05	0.39	10.8
14/06/2015	81.3	22.4	27.6	NW	NW	SW	4.8	0.14	0.06	0.33	8.8
02/07/2015	33.6	9.7	28.9	SE	SE	NW	17.5	0.05	0.02	0.46	20.2
26/07/2015	69.2	18.8	27.2	NW	SE	NW	5.5	0.12	0.06	0.29	9.0
01/08/2015	46.9	12.4	26.4	SE	SE	SE	3.7	0.18	0.09	0.31	6.1
19/08/2015	20.4	4.0	19.6	NW	NW	SE	5.1	0.14	0.07	0.32	7.4
25/08/2015	5.0	0.6	12.0	NW	SW	SE	7.7	0.13	0.11	0.56	8.5
01/09/2015	106.6	32.2	30.2	NE	NE	SW	2.5	0.23	0.11	0.26	4.90
06/09/2015	64.5	15.4	23.9	S	S	S	2.5	0.26	0.13	0.32	4.3
12/09/2015	69.3	21.4	30.9	SW	SE	NW	4.2	0.15	0.08	0.34	7.1
18/09/2015	55.3	2.3	4.2	SE	NW	SE	0.6	0.66	1.77	0.35	2.5
30/09/2015	43.3	1.0	2.3	SE	SE	SE	1.6	0.32	1.77	0.14	3.4
06/10/2015	127.9	27.5	21.5	SW	SW	SW	1.0	0.58	0.16	0.19	2.1
12/10/2015	60.0	3.8	6.3	SW	SW	SW	0.6	0.83	0.88	0.29	1.8
18/10/2015	77.4	8.6	11.1	SW	SW	SW	4.0	0.16	0.10	0.36	6.9
05/11/2015	49.9	3.0	6.0	S	SE	SW	0.4	1.51	1.77	0.07	0.78
17/12/2015	135.9	25.0	18.4	SW	SW	SW	2.2	0.32	0.05	0.18	3.3
29/12/2015	85.1	5.0	5.9	S	SW	S	10.1	0.16	0.04	0.12	6.5
28/01/2016	88.9	5.0	5.6	S	S	S	12.3	0.12	0.03	0.14	8.5
Average	70.32	17.04	24.2								

*Values in bold represent violations of WHO daily AQG
**Elemental ratios are discussed in section 3.4.

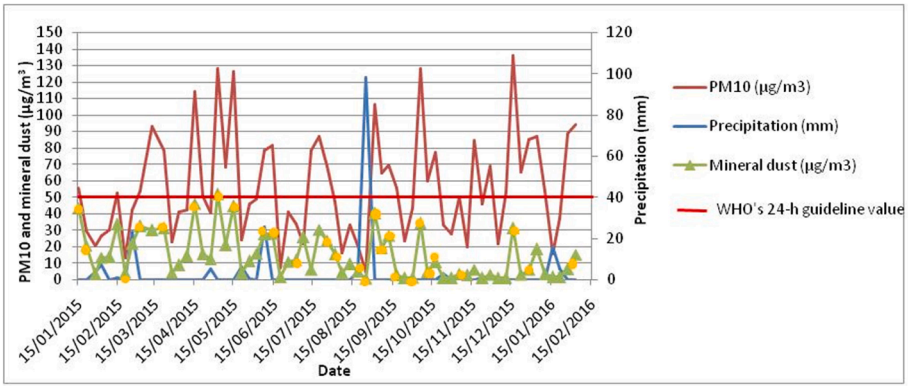

Fig. 3. Time series of the average daily PM10 concentrations with the temporal variability of the total MD and precipitation volumes for the study period.

Table 3
Average concentrations of PM10 and MD (μg/m^3) during the whole campaign (SD days and non SD days).

	Number of days	Average PM10	Average MD concentration	% MD/ PM10
SD days	27	70.3	17.05	24.25
Non SD days	37	46.8	8.2	17.52
Whole sampling period	64	56.0	11.89	21.23

winds), particles are resuspended into the atmosphere with dust aerosols. Hourly average wind speeds and frequencies of winds blowing from 16 directions taking into account only the SD days and non SD days are graphically represented in Fig. 5 (a, b) respectively. The frequency of east-south-easterly to west-south-westerly air masses likely to carry SD was 30% on SD days, while it was only 18.79% for non SD days. The influence of the sources in these directions was particularly pronounced on SD days.

The concentration roses of MD shown in Fig. 6 (a, b) during SD days and non SD days can provide useful information into the distribution of emission sources around the sampling site. As this method does not discriminate local from distant sources, five-day back trajectories allowed identifying distant sources in the WSW wind sector in which the Sahara was a potential source of MD (Fig. 2, b and c). Backward air mass trajectories also indicate SD arriving at the sampling site in the WNW to NW wind sectors (Fig. 2, a and c). Fig. 6 shows clearly that the influence of emission sources in the ESE to WSW sectors are much greater during SD days compared to non SD days. Moreover, it corroborates the major influence reported in Table 2 of the NW and SW wind sectors.

Table 4 summarizes the daily average values of temperature and wind speed on SD and non-SD days. The average ambient temperature was higher during SD days than non SD days. The frequent simultaneous increase in temperature levels with PM concentrations favours the

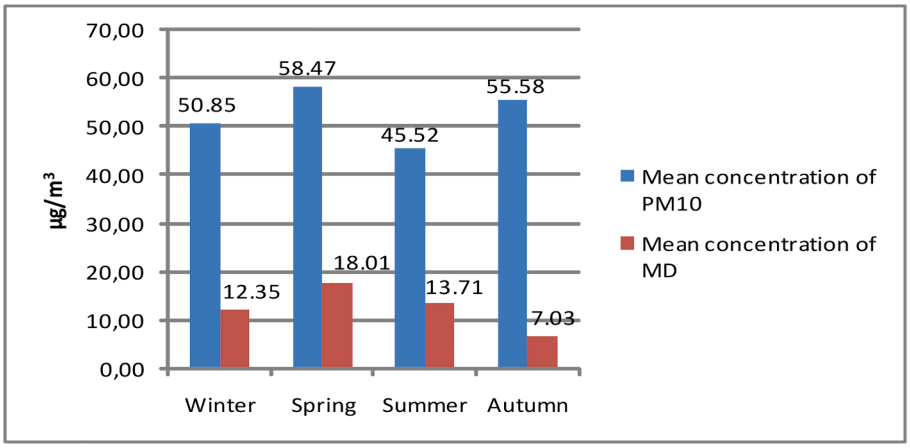

Fig. 4. The average concentration of PM10 particles and MD depending on the season.

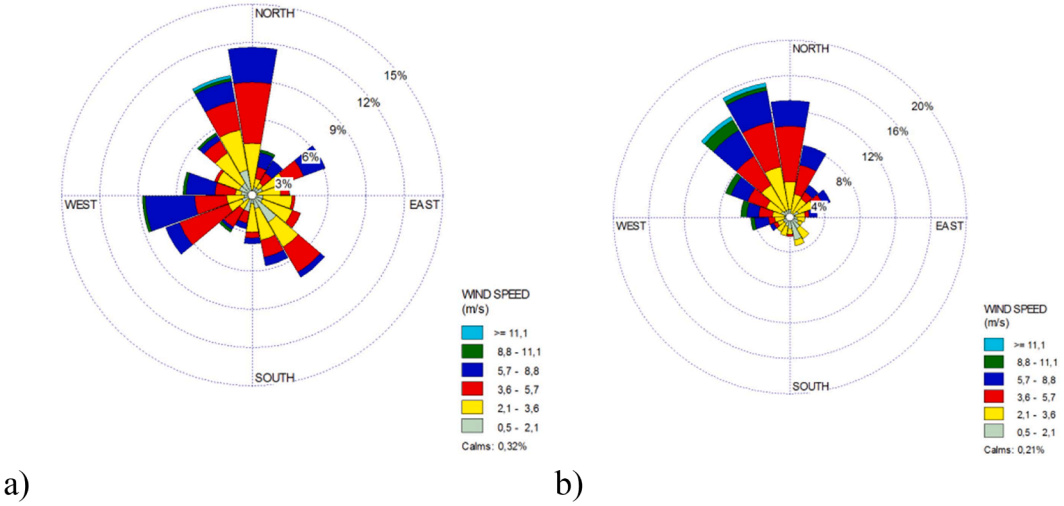

Fig. 5. Wind roses for a) SD days and b) non SD days.

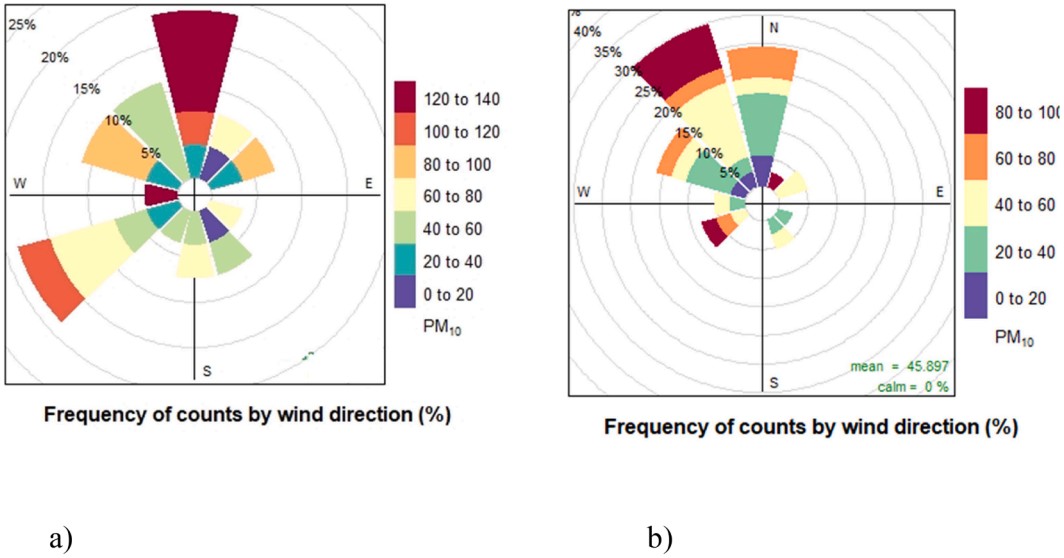

Fig. 6. Concentration roses for SD days (a) and non SD days (b).

Table 4
Average mean values of meteorological parameters on SD and no SD days.

	Temperature (° C)	Average wind speed (m/s)
SD days	18.81	3.1
Non SD days	12.05	3.4

turbulence dynamics in arid areas (Rodríguezet al., 2002). According to Pederzoliet al. (2010), high air temperatures make the dust lifting and transport easier. The average wind speed observed at the nearby weather station was higher on non SD days. This implies that MD during non SD days was more of local origin while MD during SD days was associated with long-range transport of desert dust.

The mean concentrations of crustal elements, with the exception of Ca, were ranked in the same way as MD as follows: spring > summer > winter > fall (Table 5). Ca may have a mixed crustal and anthropogenic origin.

Fig. 7 (a, b) shows the temporal variability of the daily concentrations of the studied metal elements. The latter were grouped according to their relative abundance in the earth's crust. Al which is the most abundant metal was used for comparison purposes (Remoundaki, 2013). Although Ca originated from both natural and anthropogenic sources, its pattern of temporal variability was very similar to those of Al and Fe suggesting the likely predominance of its natural character. The similarity in the temporal trend of Al, K, Mg and Ti suggest that they had common crustal sources.

3.4. Elemental ratios for Saharan dust source identification

Elemental ratios are diagnostic tools usually used to identify regional differences in the composition of dust elements (Marconi et al., 2014) and also to estimate the profiles of possible sources, the origin of air masses and local source fingerprints (Arditsoglou and Samara, 2005; Kong et al., 2011). Several studies focused on elemental ratios between the elements Al, Si, Fe, Mg, K, Ca and Ti and the occurrence of SD intrusions taking into consideration that Si and Al are the dominant elements in North Africa (Marconi et al., 2014).

According to Scheuvens et al. (2013), the most useful ratios for discriminating dust source zones are Ca/Al, Mg/Al, Fe/Al and especially the elementary ratio (Ca + Mg)/Fe which shows a pronounced north–south gradient with the highest ratios in north-west Africa. While distinctions between north-African source regions are not always clear-cut, dust source areas may be derived from northwestern and northeastern source regions for (Ca + Mg)/Fe > 2, from southern Algeria for (Ca + Mg)/Fe = 0.6–1.2, from the sub-Saharan region for (Ca + Mg)/Fe < 0.85 with the exception of some samples and from source regions in the east for (Ca + Mg)/Fe = 0.8–2.2.

The Mg content in dust and soil is generally correlated with the Ca content. Thus, higher Mg/Al ratios and higher Mg enrichment factors (Mg/Al > 0.3) as well as Ca/Al ratios (>1.0) with high Ca enrichment factors have been reported for the Atlas region (Khiri et al., 2004; Moreno et al., 2006; Castillo et al., 2008). However, lower Ca contents (Ca/Al < 0.5) were analyzed in samples from central and southern Algeria and the Sahel zone (Scheuvens et al., 2013).

According to Blanco et al. (2003), when the ratio Ca/Al is higher than K/Ca and Fe/Ca ratios, the most predominant source of dust is northwestern Sahara; otherwise, the main predominant source is central Algeria, Niger, Chad or Libya. The computed average elemental ratio Ca/Al in our site was higher than the computed average ratios K/Ca and Fe/Ca. Such a result implies that the city of Constantine was affected mainly by sources from northwestern Sahara. Such a tendancy is corroborated by the ratios (Ca + Mg)/Fe > 2 for all SD days, Mg/Al > 0.3 for most SD days and Ca/Al > 1.0 (Tables 2 and 6). Chiapello et al., (1997) also reported higher Ca/Al ratios and low K/Al and Fe/Ca ratios in dust originating from the north and west Sahara in comparison with dust from Sahel, south and central Sahara at Sal Island.

According to Table 6, Al/Fe, Fe/Ca and K/Ca ratios were higher in days affected by Saharan desert dust, while Ca/Al was more significant in days not affected by SD. This result is in accordance with the findings of Bonelli et al. (1996), Marenco et al. (2006) and Nava et al. (2012).

Table 5
Seasonal variability of MD mean crustal elements concentrations (μg/m^3).

Season	A l	Fe	Ca	K	Mg	Ti
Winter	0.42	0.35	4.05	0.18	0.20	0.02
Spring	0.76	0.48	4.90	0.23	0.32	0.04
Summer	0.66	0.42	3.08	0.21	0.21	0.04
Fall	0.41	0.28	0.89	0.15	0.08	0.02

3.5. Enrichment factors and inter-species correlation

Fig. 8 shows the enrichment factors of the main MD components in PM10.

Elements Al, Fe, K, Mg and Ti were of crustal origin since their EFs < 5. Ca has a mixed origin since 100 > EF > 5. Potential sources of MD components are shown in Table 7. It is often difficult to separate between soil dust and crustal elements as their composition is often quite similar. MD can be thought of being mainly composed of natural crustal components. Soil resuspension may include elements that originate partly from anthropogenic activities. This is the case for Ca which may derive from mineral industries such as cement and brick plants, construction and demolition works, vehicular emissions and steel plants (Bencharif-Madani et al., 2019).

Table 8 shows the correlation coefficients between the major elements constituting MD derived from the data during the whole sampling period. Elements Al, Fe, K, Mg, Ca and Ti were highly correlated and all of them correlated well with MD.

The correlation of MD with various metal elements was best in the following descending order: Fe, Mg, Ti, Al, Ca, and K (0.67–0.98). Such strong correlations imply that these elements have a common crustal origin, which is consistent with their EF values.

3.6. Enhancement of PM10 and associated metal elements during SD episodes

MD particles are the typical dominant compounds of PM10 during SD outbreaks but the anthropogenic contribution may be significant. One of the main reasons for the increase of PM10 and associated metal elements concentrations is the decrease of the thickness of the PBL (planetary boundary layer) during dust outbreaks. According to Querolet al., (2019), PBL height is gradually reduced as the intensity of the dust outbreaks increases due to the lower incident radiation reaching the surface, thermal inversions or subsidence flows, thereby causing accumulation of anthropogenic local pollutants and promoting increased concentrations. Moreover, anthropogenic pollution sources such as traffic and industrial emissions may contaminate Saharan desert dust (Castillo et al., 2008).

Heavy metals and arsenic are particulate-bonded inorganic pollutants released in the atmosphere by biogenic or industrial processes such as metallurgical process, garbage incineration and combustion of fossil fuels, mining activities, and many more. They can be long-range transported and released in the ambient air through wind-blown dust (Pasias et al., 2013). MD can pick up and transport anthropogenic material pollutants as a result of particulate/pollutant aerosolization and the absorption of such materials as heavy metals (Goudie, 2014). Moreover, the resulting increase in airborne PM levels might be enhanced by the resuspension of soil dust in the presence of winds.

Fig. 9 shows elemental concentrations in dusty and non dusty days. The concentrations of PM10 and most metal elements were enhanced by SD intrusions. The highest impact of SD intrusions was obviously observed on Al, Ca, Fe, K, Si and Ti which all represent the principal

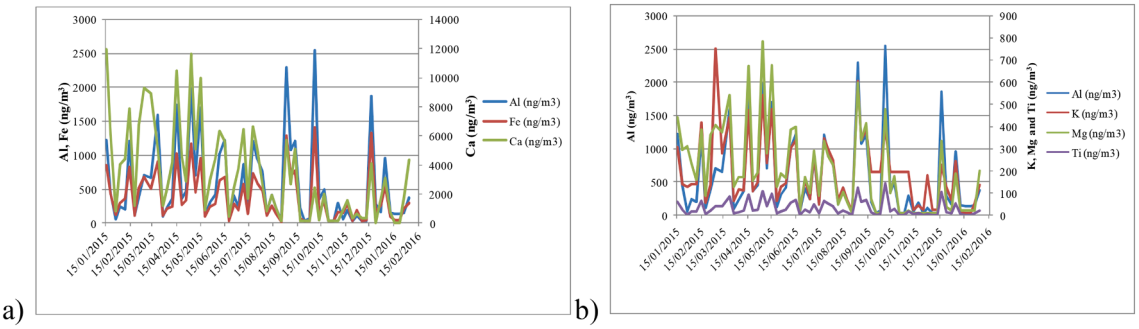

Fig. 7. Temporal variability of a) Al, Fe, and Ca and b) Al, K, Mg and Ti concentrations.

Table 6
Average elemental ratios computed from Constantine PM10 samples for days affected by Saharan desert dust (SDD) and days not affected by Saharan desert dust (NSDD).

Ratios	SDD (average)	NSDD (average)
Al/Fe	1.57	1.27
Ca/Al	5.01	8.26
Fe/Ca	0.13	0.1
K/Ca	0.07	0.05
Mg/Al	0.32	0.44
K/Al	0.31	0.49

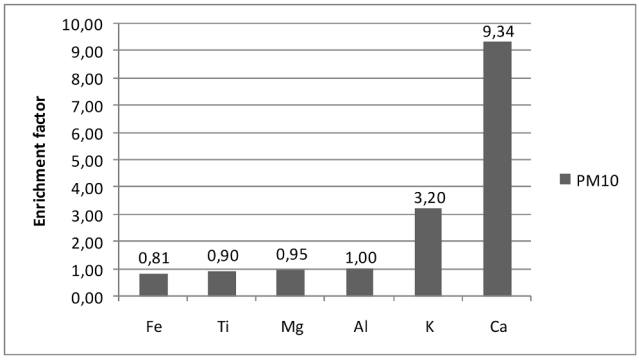

Fig. 8. Enrichment factors of main MD components.

Table 7
Sources of metal elements in mineral dust (Bencharif-Madani et al., 2019).

Elements	Possible sources
Ca, Al, Ti, Fe, Mg	Crustal, soil dust resuspension
K	Crustal

Table 8
The correlation coefficients (r^2) observed between major metal elements and the MD.

	Al	Ca	Fe	K	Mg	Ti	MD
Al	1.00						
Ca	0.67	1.00					
Fe	0.98	0.74	1.00				
K	0.80	0.72	0.81	1.00			
Mg	0.88	0.86	0.89	0.83	1.00		
Ti	1.00	0.76	0.98	0.87	0.91	1.00	
MD	0.95	0.87	0.96	0.85	0.96	0.96	1.00

components of crustal elements (Loy et al., 2000) usually used for computing MD concentrations. Potential tracers of MD in Barcelona were Fe, Cu, Ti, P, Mn, Ba, Sb, Zr, Cr whose concentrations in PM10-2.5 increased during Saharan dust days (Perez et al., 2008). An increase of the concentrations of Ti, Rb, Nb, La, Ce and Nd in PM10 in the city of Cartagena in the south-east of Spain was reported by Negral et al. (2008) from February 25, 2004 to March 15, 2005. Elements which underwent an increase during Saharan dust advections in Tenerife, Canary Islands, from 2002 to 2008 included Ca, Fe, K, Mg, V, Ni, La, Co, Cr, Fe, K, Mg, Ca, Na, La, Ti, P, V, Mn, Sr, Co, As, Pb and Ni (Rodríguez et al., 2011). Formenti et al. (2008) observed higher mean concentrations for major elements Na, Mg, Al, Si, P, S, K, Ca, Ti, and Fe on days with more intense Saharan intrusions over Niger during winter (november–december 2006) and august 2006. In addition to crustal elements, concentrations of toxic elements such as Cr, Ba, Mn, V, Mo, Se, Co, Cu, Cd, Zn, Ni and As have also increased during SD days.

According to Querolet al., (2019), minerals typically present in desert dust in the form of aluminium silicates, carbonates, oxides, salts and phosphates are rich in Al, K, Mg, Fe, Na, Ca, Ti, S and P (ratios from 1.23 to 2.94). In this study, rare earth elements underwent an increase ranging from 1.29 to 2.89. The concentrations of heavy elements classified as priority pollutants such as Sb, As, Cd, Cr, Cu, Ni, Se, Zn and Pb also increased during SD intrusions. Metal elements concentrations increased by a factor ranging from 1.05 to 3.33 with the exception of Ba for which the ratio of concentrations was 16.97. However, metal elements for which the ratios < 1 such as Na (Fig. 8a), Cs (Fig. 8d) and Tl (Fig. 8e) were not enriched by the presence of SD.

Indeed, low correlation coefficients were noted between MD and Na (0.18),

Cs (-0.18) and Tl (-0.04). Na is a marine aerosol and has a partial mineral origin while Ce is a clay-related element (Pey et al., 2013). Tl is a typical indicator of road dust (Perez et al., 2008).

4. Conclusion

This work focused on the contribution of MD to PM10 concentration levels at an urban site in Constantine, Algeria. The WHO's 24-h guideline value was exceeded on 33 days, that is 51.5% of the sampling period. Peak 24-h concentrations of MD contribution to PM10 reached 136 μg/m^3. To estimate the MD concentration, the dust "oxide" model was used based on the selection of the main elements found in the earth's crust: Al, Si, Fe and Ca, as well as other significant constituents such as K, Mg and Ti.

In order to identify the anthropogenic or crustal origin of MD constituents, average enrichment factors (EF) were estimated in PM10 at the monitoring site. Elements Al, Fe, K, Mg and Ti had a predominant crustal origin (EF < 5), excepted Ca which had a mixed MD source (EF > 5).

MD exhibited significant positive correlations with all elemental mass concentrations suggesting a possibly common natural origin. Moreover, significant positive correlations were found between all elements which are all soil-derived. In addition, the temporal variability of

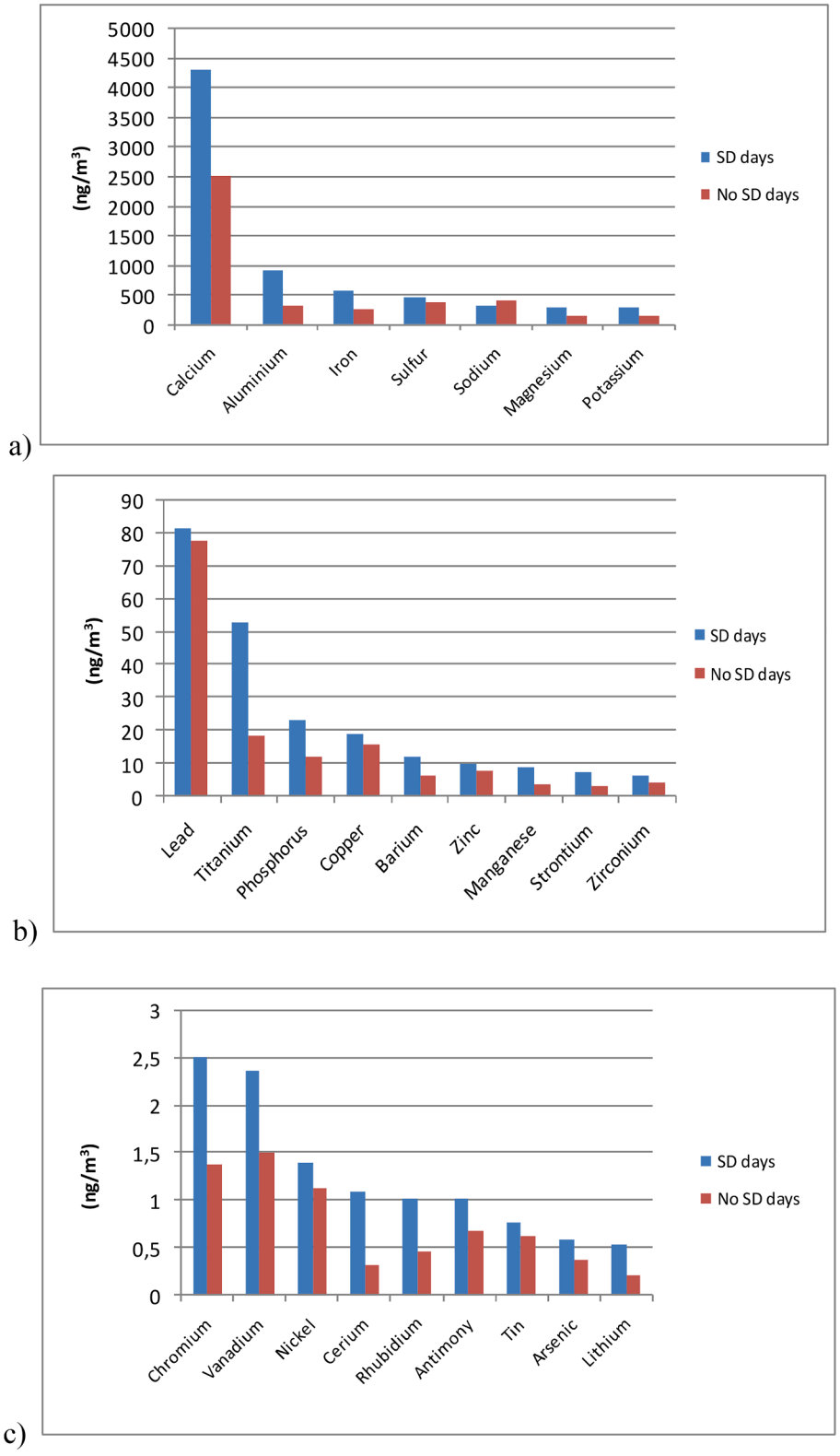

Fig. 9. Trace and major elements concentrations during SD days and non SD days.

elemental concentrations showed similar behavior corroborating the high probability of the common crustal origin of PM10 constituents.

Five-day back-trajectories using the HYSPLIT model and the prediction of dust surface concentrations through the BSC-DREAM8b model, helped to identify 27 sampling days as SD days.

Low seasonal variability of contributions of MD was observed in spring, summer and winter, while autumn exhibited the weakest contribution. The frequency of SD events during sampling days amounted to 42.2%. The subtraction of the total MD would lead to PM10 concentration of 43.8 μg/m^3. Overall, MD contributed 11.89 μg/m^3 to

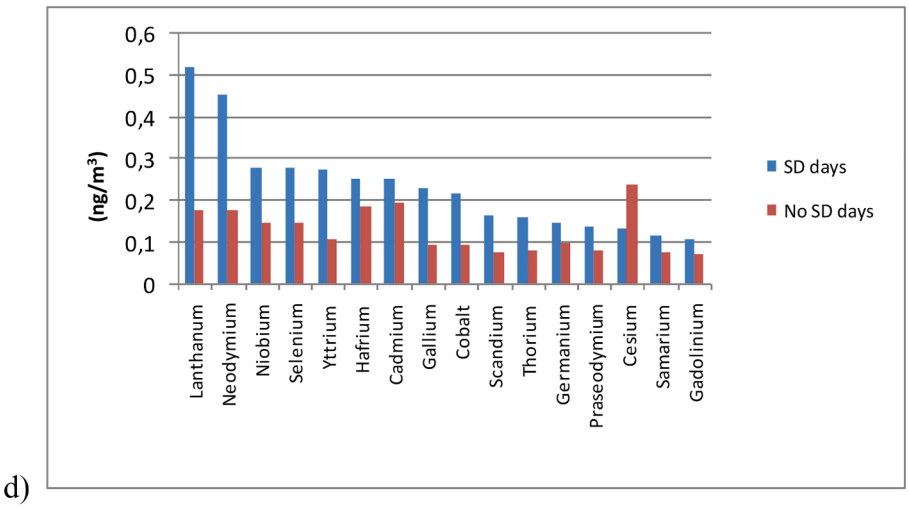

d)

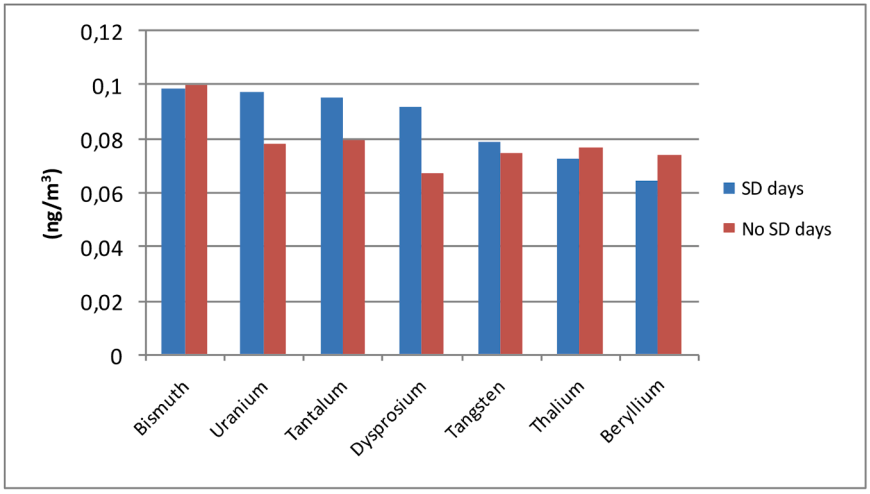

e)

Fig. 9. (*continued*).

the average PM10 concentration, while SD incursions led to an increase of 17.05 μg/m^3 in MD concentrations during SD days and 7.2 μg/m^3 throughout the whole sampling campaign.

19 days representing 29.7% of collection days were characterized by SD enhancing daily PM10 levels above the WHO daily AQG value. The contribution of MD (11.89 μg/m^3) to PM10 (56 μg/m^3) amounted to 21.23% throughout the sampling period.

The elemental ratios analysis showed that the city of Constantine was affected by SD from northwestern, southwestern and southeastern Sahara. Incursions of SD in the city of Constantine led to a remarkable increase of concentrations of all major elements and most trace elements. The use of appropriate regional background data of PM10 is recommended to provide more reliable net SD intrusions. Additional sampling should be conducted particularly when dusty events are forecasted for a better characterization of Saharan dust contribution.

Declaration of Competing Interest

The authors declare that they have no known competing financial interests or personal relationships that could have appeared to influence the work reported in this paper.

Acknowledgements

The authors gratefully acknowledge the provision of the PM10 quartz fiber filters and sample analysis support received from Professor Xavier Querol of the Institute of Environmental Assessment and Water Research (IDAEA-CSIC, Barcelona, Spain). Financial support from the DGRSDT is also acknowledged.

References

Alastuey, A., Querol, X., Castillo, S., Escudero, M., Avila, A., Cuevas, E., Torres, C., Romero, P M., Expositod, F., Garcıa, O., Diaz, J. P., Dingenen, R V.,GARCIA, O., 2005. Characterisation of TSP and PM2.5 at Izaña and Sta. Cruz de Tenerife (Canary Islands, Spain) during a Saharan Dust Episode (July 2002). Atmospheric Environment, 39(26), 4715–4728. doi:10.1016/j.atmosenv.2005.04.018.

Aleksandropoulou, V., Lazaridis, M., 2013. Identification of the influence of African dust on PM10 concentrations at the Athens air quality monitoring network during the period 2001–2010. Aerosol Air Qual. Res. 13, 1492–1503. https://doi.org/10.4209/aaqr.2012.12.0363.

Arditsoglou, A., Samara, C., 2005. Levels of total suspended particulate matter and major trace elements in Kosovo: a source identification and apportionment study. Chemosphere 59, 669–678. https://doi.org/10.1016/j.chemosphere.2004.10.056.

Barkan, J., Alpert, P., Kutiel, H., Kishcha, P., 2005. Synoptics of dust transportation days from Africa toward Italy and central Europe. J. Geophys. Res. 110, D07208. https://doi.org/10.1029/2004JD005222.

Bencharif-Madani, F., Ali-Khodja, H., Kemmouche, A., Terrouche, A., Lokorai, K., Naidja, L., Bouziane, M., 2019. Mass concentrations, seasonal variations, chemical compositions and element sources of PM10 at an urban site in Constantine, northeast Algeria. J. Geochem. Explor. 206 https://doi.org/10.1016/j.gexplo.2019.106356.

A. Blanco F. Dee Tomasi E. Filippo D. Manno M.R. Perrone A. Serra M. Tafuro A. Tepore Characterization of African dust over southern Italy Atmospheric Chemistry and Physics 3 6 2003 2147 2159 10.5194/acp-3-2147-2003.

P. Bonelli G.M. Braga Marcazzan E. Cereda Elemental composition and air trajectories of African dust transported in northern Italy S. Guerzoni R. Chester The Impact of

Desert Dust across the Mediterranean 1996 Kluwer Academic Publishers Dordrecht, The Netherlands 275 283.
C. Bouet M.T. Labiadh J.L. Rajot G. Bergametti B. Marticorena Henry des Tureaux, T., Ltifi, M., Sekraf, S., Féron, A. Impact of Desert Dust on Air Quality: What is the Meaningfulness of Daily PM Standards in Regions Close to the Sources? The Example of Southern Tunisia. Atmosphere 10 8 2019 452 10.3390/atmos10080452.
Castillo, S., Moreno, T., Querol, X., Alastuey, A., Cuevas, E., Herrmann, L., Mounkaila, M., Gibbons, W., 2008. Trace element variation in size-fractionated African desert dusts. J. Arid Environ. 72, 1034–1045.
Chiapello, I., Bergametti, G., Chatenet, B., Bousquet, P., Dulac, F., Soares, E.S., 1997. Origins of African dust transported over the northeastern tropical Atlantic. J. Geophys. Res. Atmos. 102 (D12), 13701–13709. https://doi.org/10.1029/97jd00259.
Chtioui, H., Bouchlaghem, K., Hichem Gazzah, M., 2019. Identification and assessment of intense African dust events and contribution to PM10 concentration in Tunisia. Eur. Phys. J. Plus 134 (11). https://doi.org/10.1140/epjp/i2019-13066-4.
De Longueville, F., Hountondji, Y.-C., Ozer, P., Marticorena, B., Chatenet, B., Henry, S., 2013. Saharan Dust Impacts on Air Quality: What Are the Potential Health Risks in West Africa? Human Ecol. Risk Assess. Int. J. 19 (6), 1595–1617. https://doi.org/10.1080/10807039.2012.716684.
Denier van der Gon, H., Jozwicka, M,, Hendriks, E., Gondwe, M., Schaap, M., 2000. Mineral Dust as a component of Particulate Matter. BOP – WP2 – report.
Denier van der Gon, H.A.C., Schaap, M., Visschedijk, A., Hendriks, E., 2007. A methodology to constrain the potential source strength of various soil dust sources contributing to atmospheric PM10 concentrations. Landbauforschung Völkenrode: Sonderheft, Band 308 ISBN: 978-3-86576-032-6, ISSN: 0376-0723.
E. Diapouli M.I. Manousakas S. Vratolis V. Vasilatou S. Pateraki K.A. Bairachtari X. Querol F. Amato A. Alastuey A.A. Karanasiou F. Lucarelli S. Nava C. Giulia V.L. Gianelle C. Colombi C. Alves D. Custódio C. Pio C. Spyrou G.B. Kallos K. Eleftheriadis AIRUSE-LIFE+: estimation of natural source contributions to urban ambient air PM10 and PM2.5 concentrations in southern Europe – implications to compliance with limit values Atmospheric Chemistry and Physics 17 2017 3673 3685 10.5194/acp-17-3673-2017.
European Commission, 2011. Commission Staff Working Paper Establishing Guidelines for Determination of Contributions From the Re-suspension of Particulates Following Winter Sanding or Salting of Roads Under the Directive 2008/50/EC on Ambient Air Quality and Cleaner Air for Europe. vol. 207. European Commission, SEC 2011. 43 pp. http://ec.europa.eu/environment/air/quality/legislation/pdf/sec_2011_0207.pdf.
M. Escudero S. Castillo X. Querol A. Avila M. Alarcon M.M. Viana A. Alastuey E. Cuevas S. Rodrıguez Wet and dry African dust episodes over Eastern Spain J. Geophys. Res. 110, D18S08 2005 2005 10.1029/2004JD004731.
Escudero, M., Querol, X., Ávila, A., Cuevas, E., 2007a. Origin of the exceedances of the European daily PM limit value in regional background areas of Spain. Atmos. Environ. 41 (4), 730–744. https://doi.org/10.1016/j.atmosenv.2006.09.014.
M. Escudero X. Querol J. Pey A. Alastuey N. Pérez F. Ferreira S. Alonso Rodríguez, S., Cuevas, E., Rodríguez, S., Alonso, S. A methodology for the quantification of the net African dust load in air quality monitoring networks Atmospheric Environment 41 26 2007 5516 5524 10.1016/j.atmosenv.2007.04.047.
Flores, R.M., Kaya, N., Eşer, Ö., Saltan, Ş., 2017. The effect of mineral dust transport on PM 10 concentrations and physical properties in Istanbul during 2007–2014. Atmos. Res. 197, 342–355. https://doi.org/10.1016/j.atmosres.2017.07.009.
P. Formenti J.L. Rajot K. Desboeufs S. Caquineau S. Chevaillier S. Nava A. Gaudichet E. Journet S. Triquet S. Alfaro M. Chiari J. Haywood H. Coe E. Highwood Regional variability of the composition of mineral dust from western Africa: Results from the AMMA SOP0/DABEX and DODO field campaigns Journal of Geophysical Research 113 2008 10.1029/2008jd009903.
Gerasopoulos, E., Kouvarakis, G., Babasakalis, P., Vrekoussis, M., Putaud, J., Mihalopoulos, N., 2006. Origin and variability of particulate matter (PM10) mass concentrations over the Eastern Mediterranean. Atmos. Environ. 40 (25), 4679–4690. https://doi.org/10.1016/j.atmosenv.2006.04.020.
Gobbi, G.P., Barnaba, F., Ammannato, L., 2007. Estimating the impact of Saharan dust on the year 2001 PM10 record of Rome, Italy. Atmos. Environ. 41 (2), 261–275. https://doi.org/10.1016/j.atmosenv.2006.08.036.
Goudie, A.S., 2014. Desert dust and human health disorders. Environ. Int. 63, 101–113.
Guan, Q., Luo, H., Pan, N., Zhao, R., Yang, L., Yang, Y., Tian, J., 2019. Contribution of dust in northern China to PM10 concentrations over the Hexi corridor. Sci. Total Environ. https://doi.org/10.1016/j.scitotenv.2018.12.412.
P.L. Israelevich Z. Levin J.H. Joseph E. Ganor Desert aerosol transport in the Mediterranean region as inferred from the TOMS aerosol index Journal of Geophysical Research: Atmospheres 107 D21 2002 AAC 13–1–AAC 13–13 10.1029/2001jd002011.
Jiménez, E., Linares, C., Martínez, D., Díaz, J., 2010. Role of Saharan dust in the relationship between particulate matter and short-term daily mortality among the elderly in Madrid (Spain). Sci. Total Environ. 408 (23), 5729–5736. https://doi.org/10.1016/j.scitotenv.2010.08.049.
Kabatas, B., Unal, A., Pierce, R.B., Kindap, T., Pozzoli, L., 2014. The contribution of Saharan dust in PM10 concentration levels in Anatolian Peninsula of Turkey. Sci. Total Environ. 488–489, 413–421. https://doi.org/10.1016/j.scitotenv.2013.12.045.
Kchih, H., Perrino, C., Cherif, S., 2015. Investigation of Desert Dust Contribution to Source Apportionment of PM10 and PM2.5 from a Southern Mediterranean Coast. Aerosol Air Qual. Res. 15, 454–464. https://doi.org/10.4209/aaqr.2014.10.0255.
Kemmouche, A., Ali-Khodja, H., Bencharif-Madani, F., Mahía, P.L., Querol, X., 2017. Comparative study of bulk and partial digestion methods for airborne PM10-bound elements in a high mineral dust urban site in Constantine, Algeria. Int. J. Environ. Anal. Chem. 1–19 https://doi.org/10.1080/03067319.2017.1390088.
Khiri, F., Ezaidi, A., Kabbachi, K., 2004. Dust deposits in Souss-Massa basin, South-West of Morocco: granulometrical, mineralogical and geochemical characterisation. J. Afr. Earth Sc. 39 (3–5), 459–464. https://doi.org/10.1016/j.jafrearsci.2004.07.019.
Knippertz P, 2014. Meteorological Aspects of Dust Storms, In : Mineral dust: a key player in the earth system. Knippertz, P and Stuut, J-B. (Eds.). Springer, Dordrecht 2014; 385-409. DOI 10.1007/978-94-017-8978-3.
Kong, S., Ji, Y., Lu, B., Chen, L., Han, B., Li, Z., Bai, Z., 2011. Characterization of PM10 source profiles for fugitive dust in Fushun-a city famous for coal. Atmos. Environ. 45 (30), 5351–5365. https://doi.org/10.1016/j.atmosenv.2011.06.050.
Loy, M. V., Bahadori, T., Wyzga, R., Edgerton, B. H. and E., 2000. The Aerosol Research and Inhalation Epidemiology Study (ARIES): PM25 Mass and Aerosol Component Concentrations and Sampler Intercomparisons. J. Air Waste Manag. Assoc, 50(8), 1446–1458.doi:10.1080/10473289.2000.10464187.
Maghrabi, A.H., Al-Dosari, A.F., 2016. Effects on surface meteorological parameters and radiation levels of a heavy dust storm occurred in Central Arabian Peninsula. Atmos. Res. 182, 30–35. https://doi.org/10.1016/j.atmosres.2016.07.024.
M. Marconi D.M. Sferlazzo S. Becagli C. Bommarito G. Calzolai M. Chiari A. di Sarra C. Ghedini J.L. Gómez-Amo F. Lucarelli D. Meloni F. Monteleone S. Nava G. Pace S. Piacentino F. Rugi M. Severi R. Traversi R. Udisti Saharan dust aerosol over the central Mediterranean Sea: PM10 chemical composition and concentration versus optical columnar measurements Atmospheric Chemistry and Physics 14 4 2014 2039 2054 10.5194/acp-14-2039-2014.
F. Marenco P. Bonasoni F. Calzolari M. Ceriani M. Chiari P. Cristofanelli A. D'Alessandro P. Fermo F. Lucarelli F. Mazzei S. Nava A. Piazzalunga P. Prati G. Valli R. Vecchi Characterization of atmospheric aerosols at Monte Cimone, Italy, during summer 2004: Source apportionment and transport mechanisms Journal of Geophysical Research 111 D24 2006 10.1029/2006jd007145.
Matassoni, L., Pratesi, G., Centioli, D., Cadoni, F., Malesani, P., Caricchia, A.M., di Bucchianico, A.D.M., 2009. Saharan dust episodes in Italy: influence on PM10 daily limit value (DLV) exceedances and the related synoptic. J. Environ. Monit. 11 (9), 1586. https://doi.org/10.1039/b903822a.
Matassoni, L., Pratesi, G., Centioli, D., Cadoni, F., Lucarelli, F., Nava, S., Malesani, P., 2011. Saharan dust contribution to PM10, PM2.5 and PM1 in urban and suburban areas of Rome: a comparison between single-particle SEM-EDS analysis and whole-sample PIXE analysis. J. Environ. Monit. 13 (3), 732. https://doi.org/10.1039/c0em00535e.
Monteiro, A., Fernandes, A,P., Gama, C., Borrego, C , Tchepel, O., 2015. Assessing the mineral dust from North Africa over Portugal region using BSC–DREAM8b model. Atmos. Poll. Res., 6(1), 70–81. doi:10.5094/apr.2015.009.
J.P. Miller-Schulze M. Shafer J.J. Schauer J. Heo P.A. Solomon J. Lantz M. Artamonova B. Chen S. Imashev L. Sverdlik G. Carmichael J. DeMinter Seasonal contribution of mineral dust and other major components to particulate matter at two remote sites in Central Asia Atmospheric Environment 119 11 2015 20 10.1016/j.atmosenv.2015.07.011.
Monteiro, A., Fernandes, A,P., Gama, C., Borrego, C , Tchepel, O., 2015. Assessing the mineral dust from North Africa over Portugal region usng BSC–DREAM8b model. Atmospheric Pollution Research, 6(1), 70–81. doi:10.5094/apr.2015.009.
Moreno, T., Querol, X., Castillo, S., Alastuey, A., Cuevas, E., Herrmann, L., Mounkaila, N., Elvira, J., Gibbons, W., 2006. Geochemical variations in aeolian mineral particles from the Sahara-Sahel Dust Corridor. Chemosphere 65 (2), 261–270. https://doi.org/10.1016/j.chemosphere.2006.02.052.
Naidja, L., Ali-Khodja, H., Khardi, S., 2018. Sources and levels of particulate matter in North African and Sub-Saharan cities: a literature review. Environ. Sci. Pollut. Res. https://doi.org/10.1007/s11356-018-1715-x.
Nava, S., Becagli, S., Calzolai, G., Chiari, M., Lucarelli, F., Prati, P., Traversi, R., Udisti, R., Valli, G., Vecchi, R., 2012. Saharan dust impact in central Italy: An overview on three years elemental data records. Atmos. Environ. 60, 444–452. https://doi.org/10.1016/j.atmosenv.2012.06.064.
Negral, L., Moreno-Grau, S., Moreno, J., Querol, X., Viana, M.M., Alastuey, A., 2008. Natural and Anthropogenic Contributions to PM10 and PM2.5 in an Urban Area in the Western Mediterranean Coast. Water Air Soil Pollut. 192 (1–4), 227–238. https://doi.org/10.1007/s11270-008-9650-y.
Pandolfi, M., Tobias, A., Alastuey, A., Sunyer, J., Schwartz, J., Lorente, J., Pey, J., Querol, X., 2014. Effect of atmospheric mixing layer depth variations on urban air quality and daily mortality during Saharan dust outbreaks. Sci. Total Environ. 494–495, 283–289.
Pasias, I.N., Thomaidis, N.S., Bakeas, E.B., Piperaki, E.A., 2013. Application of zirconium–iridium permanent modifier for the simultaneous determination of lead, cadmium, arsenic, and nickel in atmospheric particulate matter by multi-element electrothermal atomic absorption spectrometry. Environ. Monit. Assess. 185 (8), 6867–6879. https://doi.org/10.1007/s10661-013-3071-0.
Pederzoli, A., Mircea, M., Finardi, S., di Sarra, A., Zanini, G., 2010. Quantification of Saharan dust contribution to PM10 concentrations over Italy during 2003–2005. Atmos. Environ. 44 (34), 4181–4190. https://doi.org/10.1016/j.atmosenv.2010.07.031.
L. Perez A. Tobias X. Querol N. Künzli J. Pey A. Alastuey M. Viana N. Valero M. González-Cabre J. Sunyer Coarse Particles From Saharan Dust and Daily Mortality Epidemiology 19 6 2008 800 807 10.1097/ede.0b013e31818131cf.
Perez, L., Tobías, A., Querol, X., Pey, J., Alastuey, A., Díaz, J., Sunyer, J., 2012. Saharan dust, particulate matter and cause-specific mortality: A case–crossover study in Barcelona (Spain). Environ. Int. 48, 150–155. https://doi.org/10.1016/j.envint.2012.07.001.

M.R. Perrone A. Genga M. Siciliano T. Siciliano F. Paladini P. Burlizzi Saharan dust impact on the chemical composition of PM10 and PM1 samples over south-eastern Italy Arabian Journal of Geosciences 9(2).doi:10.1007/s12517-015-2227-3 2016.

Pey, J., Alastuey, A., Querol, X., Pérez, N., Cusack, M., 2010. simplified approach to the indirect evaluation of the chemical composition of atmospheric aerosols from PM mass concentrations. Atmos. Environ. 44 (39), 5112–5121. https://doi.org/10.1016/j.atmosenv.2010.09.009.

Pey, J., Querol, X., Alastuey, A., Forastiere, F., Stafoggia, M., 2013a. African dust outbreaks over the Mediterranean Basin during 2001–2011: PM10 concentrations, phenomenology and trends, and its relation with synoptic and mesoscale meteorology. Atmos. Chem. Phys. 13 (3), 1395–1410. https://doi.org/10.5194/acp-13-1395-2013.

J. Pey A. Alastuey X. Querol PM10 and PM2.5 sources at an insular location in the western Mediterranean by using source apportionment techniques Science of the Total Environment 456–457 2013 267 277 /10.1016/j.scitotenv.2013.03.084.

Querol, X., 2001. PM10 and PM2.5 source apportionment in the Barcelona Metropolitan area, Catalonia, Spain. Atmos. Environ. 35 (36), 6407–6419. https://doi.org/10.1016/s1352-2310(01)00361-2.

X. Querol J. Pey M. Pandolfi A. Alastuey M. Cusack Viana Pérez N., Moreno, M., Mihalopoulos, T., Kallos, N., Kleanthous, G., Kleanthous, S., African dust contributions to mean ambient PM10 mass-levels across the Mediterranean Basin Atmospheric Environment 43 28 2009 4266 4277 10.1016/j.atmosenv.2009.06.013.

X. Querol A. Tobías N. Pérez A. Karanasiou F. Amato M. Stafoggia C. Pérez García-Pando P. Ginoux F. Forastiere S. Gumy P. Mudu A. Alastuey Monitoring the impact of desert dust outbreaks for air quality for health studies Environment International 130 2019 10.1016/j.envint.2019.05.061.

Remoundaki, E., Bourliva, A., Kokkalis, P., Mamouri, R.E., Papayannis, A., Grigoratos, T., Samara, C., Tsezos, M., 2011. PM10 composition during an intense Saharan dust transport event over Athens (Greece). Sci. Total Environ. 409 (20), 4361–4372. https://doi.org/10.1016/j.scitotenv.2011.06.026.

Remoundaki, E., Papayannis, A., Kassomenos, P., Mantas, E., Kokkalis, P., Tsezos, M., 2013. Influence of Saharan Dust Transport Events on PM2.5 Concentrations and Composition over Athens. Water Air Soil Pollut, 224-1373. DOI 10.1007/s11270-012-1373-4.

Rodríguez, S., Querol, X., Alastuey, A., Kallos, G., Kakaliagou, O., 2001. Saharan dust contributions to PM10 and TSP levels in Southern and Eastern Spain. Atmos. Environ., 35(14), 2433–2447. doi:10.1016/s1352-2310(00)00496-9.

Rodríguez, S., Querol, X., Alastuey, A., Plana, F., 2002. Sources and processes affecting levels and composition of atmospheric aerosol in the western Mediterranean. J. Geophys. Res. 107, 4777. https://doi.org/10.1029/2001JD001488.

S. Rodríguez A. Alastuey S. Alonso-Pérez X. Querol E. Cuevas J. Abreu-Afonso M. Viana P. Pérez N., Pandolfi, M., de la Rosa, J. Transport of desert dust mixed with North African industrial pollutants in the subtropical Saharan Air Layer. Atmos. Chem. Phys. 11 13 2011 6663 6685 10.5194/acp-11-6663-2011.

Salvador, P., Artíñano, B., Molero, F., Viana, M., Pey, J., Alastuey, A., Querol, X., 2013. African dust contribution to ambient aerosol levels across central Spain: Characterization of long-range transport episodes of desert dust. Atmos. Res. 127, 117–129. https://doi.org/10.1016/j.atmosres.2011.12.011.

Salvador, P., Alonso-Pérez, S., Pey, J., Artíñano, B., de Bustos, J.J., Alastuey, A., Querol, X., 2014. African dust outbreaks over the western Mediterranean Basin: 11-year characterization of atmospheric circulation patterns and dust source areas. Atmos. Chem. Phys. 14 (13), 6759–6775. https://doi.org/10.5194/acp-14-6759-2014.

Schepanski, K., Tegen, I., Todd, M. C., Heinold, B., Bönisch, G., Laurent, B., Macke, A., 2009. Meteorological processes forcing Saharan dust emission inferred from MSG-SEVIRI observations of subdaily dust source activation and numerical models. Journal of Geophysical Research, 114(D10).doi:10.1029/2008jd010325.

Scheuvens, D., Schütz, L., Kandler, K., Ebert, M., Weinbruch, S., 2013. Bulk composition of northern African dust and its source sediments — A compilation. Earth Sci. Rev. 116, 170–194. https://doi.org/10.1016/j.earscirev.2012.08.005.

Scheuvens, D., Schütz, L., Kandler, K., Ebert, M., Weinbruch, S., 2013. Bulk composition of northern African dust and its source sediments — A compilation. Earth Sci. Rev. 116, 170–194. https://doi.org/10.1016/j.earscirev.2012.08.005.

Stafoggia, M., Zauli-Sajani, S., Pey, J., Samoli, E., Alessandrini, E., Basagaña, X., Cernigliaro, A., Chiusolo, M., Demaria, M., Díaz, J., Faustini, A., Katsouyanni, K., Kelessis, A.G., Linares, C., Marchesi, S., Medina, S., Pandolfi, P., Pérez, N., Querol, X., Randi, G., Ranzi, A., Tobias, A., Forastiere, F. and the MED-PARTICLES Study Group Desert Dust Outbreaks in Southern Europe: Contribution to Daily PM10 Concentrations and Short-Term Associations with Mortality and Hospital Admissions Environmental Health Perspectives 124 4 2016 413 419 doi.org/10.1289/ehp.1409164.

Sudheer, A.K., Rengarajan, R.A., 2012. Atmospheric mineral dust and trace metals over urban environment in Western India during winter. Aerosol Air Qual. Res. 12, 923–933. https://doi.org/10.4209/aaqr.2011.12.0237.

Talbi, A., Kerchich, Y., Kerbachi, R., Boughedaoui, M., 2017. Assessment of annual air pollution levels with PM1, PM2.5, PM10 and associated heavy metals in Algiers, Algeria. Environ. Pollut. 232, 252–263. https://doi.org/10.1016/j.envpol.2017.09.041.

Taylor, S.R., McLennan, S.M., 1995. The Geochemical Evolution of the Continental Crust. Rev. Geophys. 33 (2), 241–265.

Terrouche, A., Ali-Khodja, H., Kemmouche, A., Bouziane, M., Derradji, A., Charron, A., 2015. Identification of sources of atmospheric particulate matter and trace metals in Constantine, Algeria. Air Qual. Atmos. Health 9 (1), 69–82. https://doi.org/10.1007/s11869-014-0308-1.

Thorsteinsson, T., Gísladóttir, G., Bullard, J., McTainsh, G., 2011. Dust storm contributions to airborne particulate matter in Reykjavík, Iceland. Atmos. Environ. 45 (32), 5924–5933. https://doi.org/10.1016/j.atmosenv.2011.05.023.

Valido, H.I., Padoan, E., Moreno, T., Querol, X., Font, O., Amato, F., 2018. Physico-chemical characterization of playground sand dust, inhalable and bioaccessible fractions. Chemosphere 190, 454–462. https://doi.org/10.1016/j.chemosphere.2017.09.101.

Wang, Z., Pan, X., Uno, I., Chen, X., Yamamoto, S., Zheng, H., Li, J., Wang, Z., 2018. Importance of mineral dust and anthropogenic pollutants mixing during a long-lasting high PM event over East Asia. Environ. Pollut. 234, 368–378. https://doi.org/10.1016/j.envpol.2017.11.068.

WHO, 2016. Ambiant Air Pollution: a Global Assessment of Exposure and Burden of Disease ISBN 978 92 4 151135 3.